Supporting Information

Enhanced Hyaline Cartilage Formation and Continuous Osteochondral Regeneration via 3D-Printed Heterogeneous Hydrogel with Multi-Crosslinking Inks

Zhonglian Wu [a], Hang Yao [a*], Haidi Sun [a], Zehao Gu [a], Xu Hu [b], Jian Yang [c], Junli Shi [a], Haojun Yang [d], Jihang Dai [e], Hui Chong [a], Dong-An Wang [b], Liwei Lin [f,g*], Wang Zhang [a,g*]

[a] School of Chemistry and Chemical Engineering, Yangzhou University, Yangzhou, Jiangsu 225009, P. R. China

[b] Department of Biomedical Engineering, City University of Hong Kong, Kowloon Tong, Hong Kong SAR 999077, P.R. China

[c] Clinical Medical College, Yangzhou University, Yangzhou, Jiangsu 225001, P. R. China.

[d] The Affiliated Changzhou No. 2 People's Hospital of Nanjing Medical University Changzhou, Jiangsu 213004, P. R. China.

[e] Department of Orthopedics and Sports Medicine, Northern Jiangsu People's Hospital, Yangzhou, Jiangsu 225001, P. R. China

[f] School of Petrochemical Engineering, Changzhou University, Changzhou, Jiangsu 213164, P. R. China

[g] Department of Applied Bioengineering, Graduate School of Convergence Science and Technology, Seoul National University, Seoul 08826, Republic of Korea

*Co-Corresponding Authors:

Hang YAO, Ph.D.

School of Chemistry and Chemical Engineering

Yangzhou University

Yangzhou 225009, P. R. China

Email: yaohang@yzu.edu.cn (H. Yao)

Liwei LIN, Ph.D.

School of Petrochemical Engineering

Changzhou University

Changzhou, 213164, P. R. China

Email: lin-official@snu.ac.kr (L. Lin)

Wang ZHANG, Ph.D.

School of Chemistry and Chemical Engineering

Yangzhou University

Yangzhou 225009, P. R. China

Email: zhangwang@yzu.edu.cn; zhangwang@snu.ac.kr (W. Zhang)

Experimental section

Preparation of printing inks

The main components of the extracellular matrix (ECM) in articular cartilage are proteoglycan and type II collagen. Subchondral bone is mainly composed of type I collagen, proteoglycans, and hydroxyapatite. To accurately simulate osteochondral tissue, sodium alginate (SA) and decellularized natural cartilage(dNC) were chosen as the upper-layer inks. The GelMA, SA, and nano-hydroxyapatite(nHA) were chosen as the lower-layer ink. The following ink ratio was determined according to the relevant literature and the preliminary experiment results [1-5].

Preparation of the upper-layer inks: A 5% w/v SA solution was mixed with 0.01, 0.02, and 0.04 mol/L $CaCl_2$ solution. Meanwhile, 15% w/v dNC (<150 μm) and 5% w/v SA solutions were mixed with 0.01, 0.02, and 0.04 mol/L $CaCl_2$ solution separately. The prepared solutions were placed in a refrigerator at 4 °C overnight for degassing.

Preparation of lower-layer inks: 0.02 mol/L $CaCl_2$, 0.5% w/v I-2959, and 5% w/v SA were added to a 10% w/v GelMA solution to obtain Gel-SA solution. Subsequently, 2% (w/v) nHA was added to the Gel-SA solution to obtain the Gel@nHA-SA solution.

Cell culture

Chondrocytes were isolated from porcine articular cartilage tissues according to our previously reported protocol [6]. The cells were then cultured in high-glucose DMEM supplemented with 10% FBS and 1% PS in a cell incubator (5% CO_2, 37 °C). Passage 2 of the cartilage cells was used in follow-up cell experiments.

Rat bone marrow-derived mesenchymal stem cells (rBMSCs) were isolated by removing the femur ends and flushing the marrow. The cells were cultured in DMEM with low glucose, 10% FBS, and 1% PS in a cell incubator (5% CO_2, 37 °C). Passages 3 and 4 of the BMSCs were used in this study.

Supplementary Data

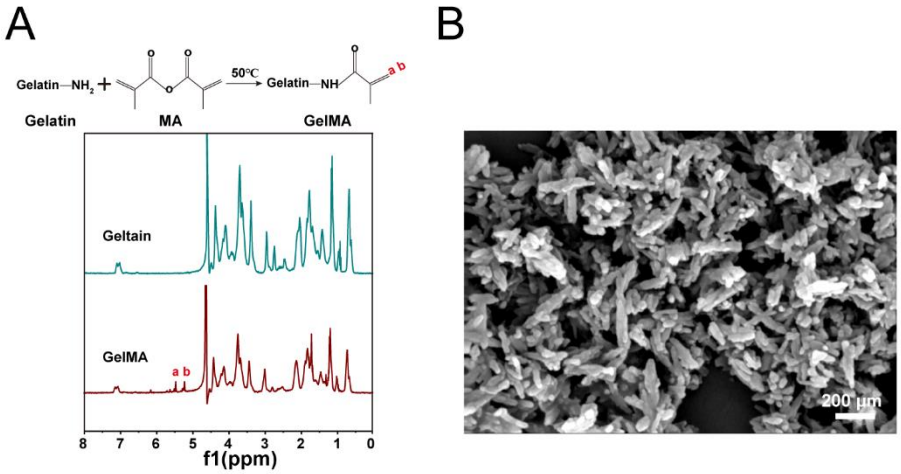

Figure S1. A) ^{1}H-NMR spectra of gelatin and GelMA. The chemical shift between 5 and 6 ppm in the spectrum of GelMA showed the double bond formation. B) The SEM image. Scale bar: 200 nm.

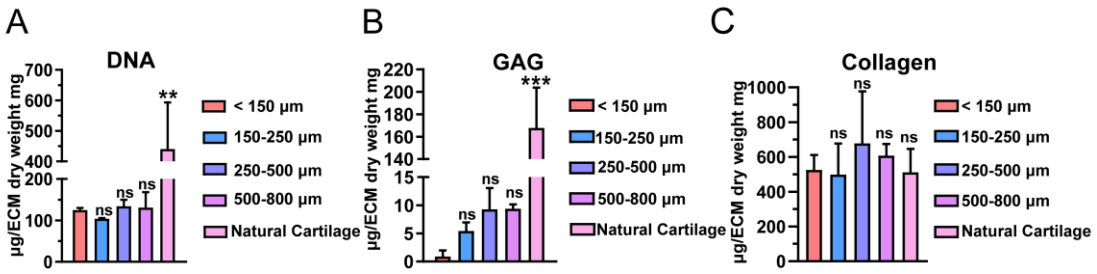

Figure S2. Decellularized natural cartilage (dNC) of different sizes is compared with Natural Cartilage (NC). A-C) Quantification of DNA residue, GAG, and total collagen contents in dNC of different sizes and NC. The data were analyzed by one-way ANOVA analysis, and error bars indicate Mean ± SD, *p<0.05, **p<0.01, ***p<0.001.

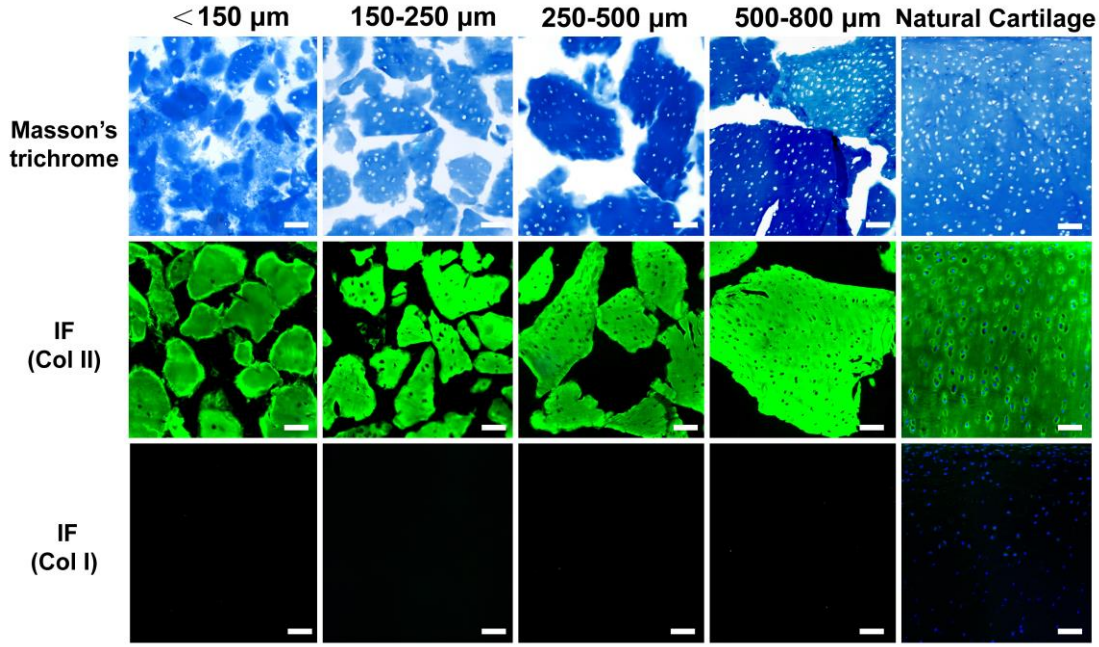

Figure S3. Histology of dNC of different sizes and NC was conducted using Masson's trichrome staining and Immunofluorescence (IF) staining with antibodies targeting collagen type II (COL II) and collagen type I (COL I). Positive IF stain manifests as emitting green fluorescence, while positive DAPI staining of cell nuclei is observed as emitting blue fluorescence. Scale bar: 100 μm.

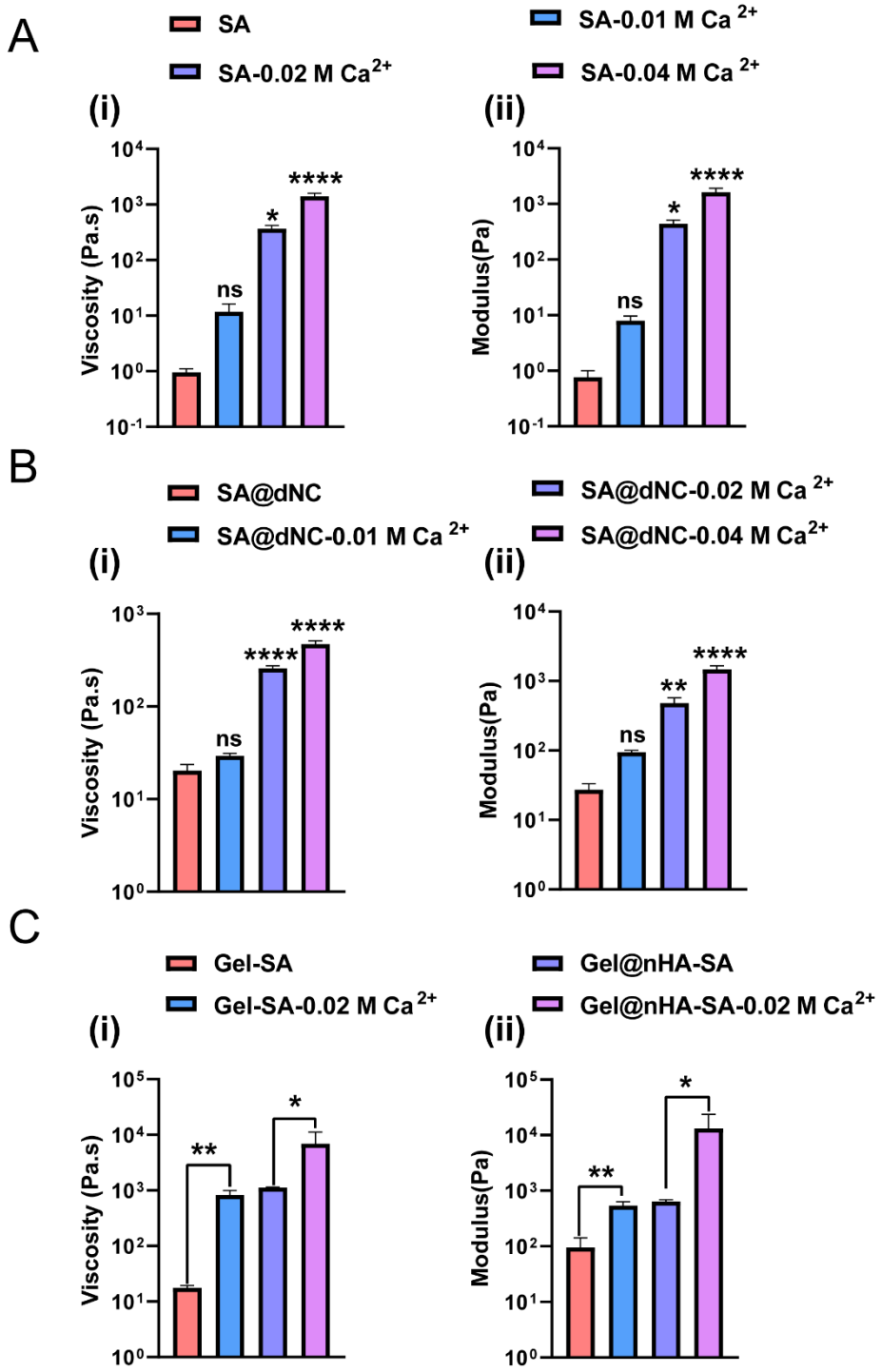

Figure S4. Rheological properties of the printing inks. A, B) Viscosity (i) and modulus (ii) of SA and SA@dNC inks with different pre-crosslinking degrees were quantitatively analyzed at 25 ℃. C) Viscosity (i) and modulus (ii) of Gel–SA and Gel@nHA–SA inks with different pre-crosslinking degrees were quantitatively analyzed at 37 ℃. All data of the viscosity were quantified at share rate of 0.1 1/s. All modulus data represented the storage modulus (G′). The data were analyzed by one-way analysis of variance (ANOVA), and error bars indicate mean ± standard deviation (SD), *$p < 0.05$, **$p < 0.01$, and ***$p < 0.001$. "ns" represented no significance.

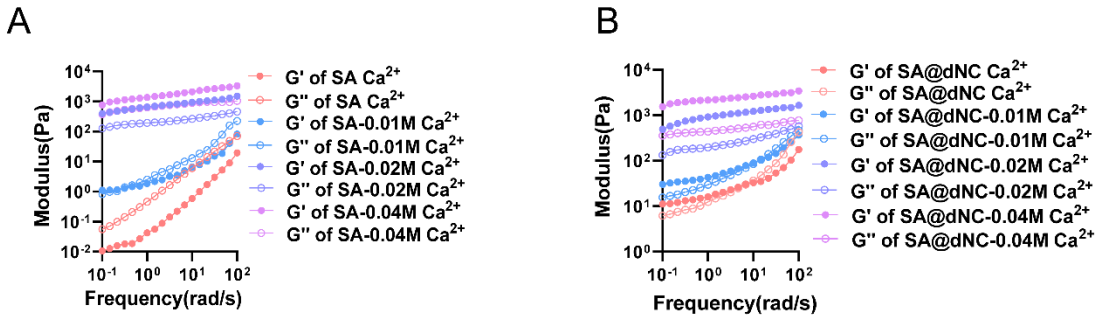

Figure S5. Rheological properties of upper layer inks. A-B) Storage modulus(G′) and loss modulus (G″) change of SA and SA@dNC inks of different pre-crosslinking degrees were analyzed over a frequency range of 0.1–100 rad/s at 25℃.

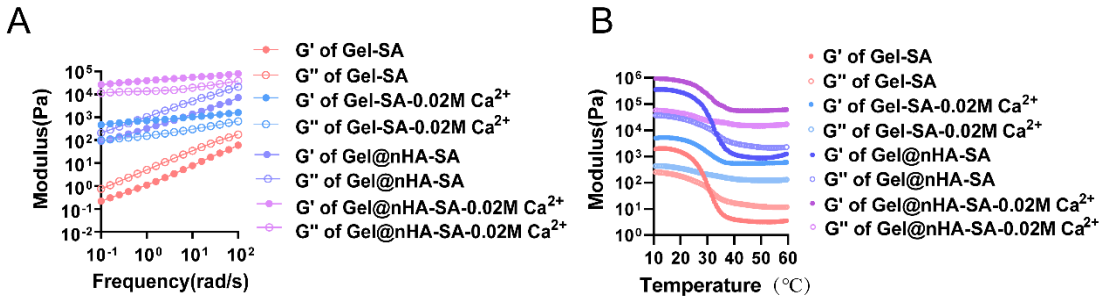

Figure S6. Rheological properties of lower layer inks. A) G′ and G″ change of Gel-SA and Gel@nHA-SA inks of different pre-crosslinking degrees were analyzed over a frequency range of 0.1 – 100 rad/s at 37 ℃. B) G′ and G″ change of low layer inks of different pre-crosslinking degrees according to the temperature range of 10 – 60 ℃.

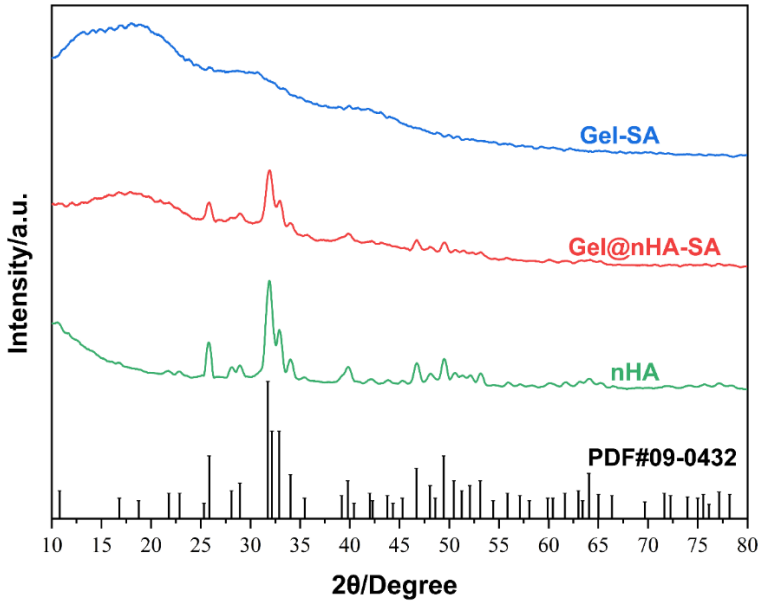

Figure S7. XRD image of lower layer hydrogel (Gel-SA, Gel@nHA-SA) inks.

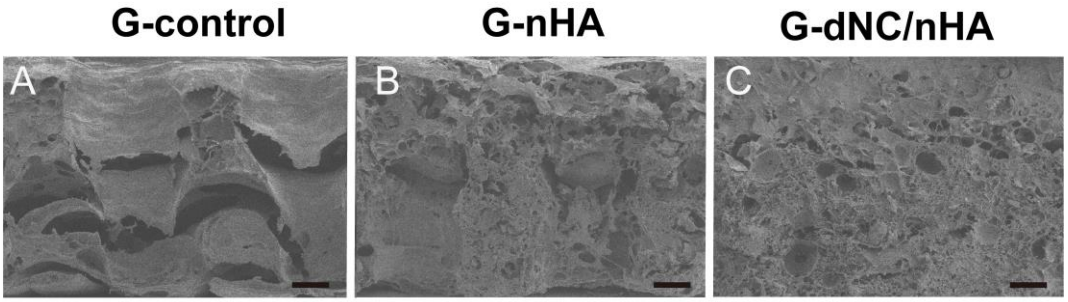

Figure S8. The cross-section SEM images of the bilayer hydrogel scaffold. Scale bar:100 μm.

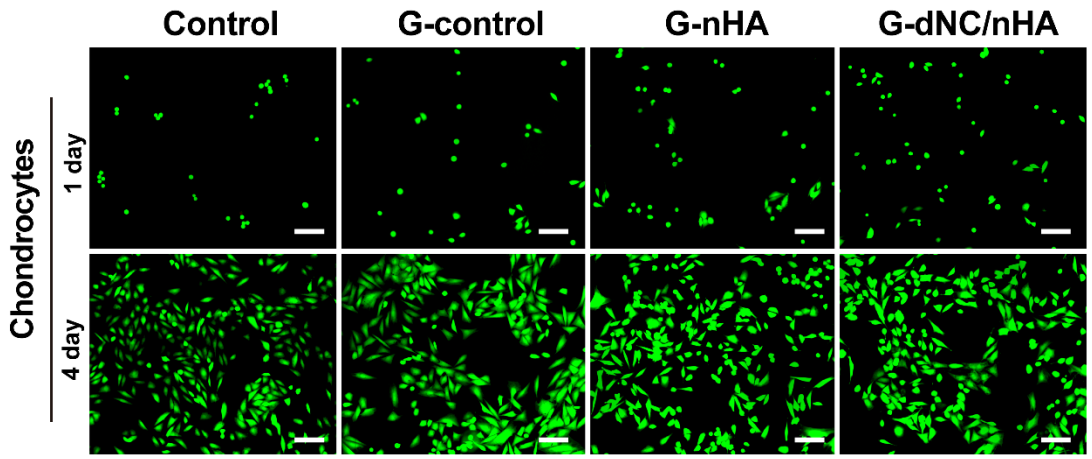

Figure S9. Images of Live/Dead staining were captured after co-culturing Chondrocytes with various samples for 1 and 4 days. (Live cells: green fluorescence, dead cells: red fluorescence. Scale bar:100 μm.

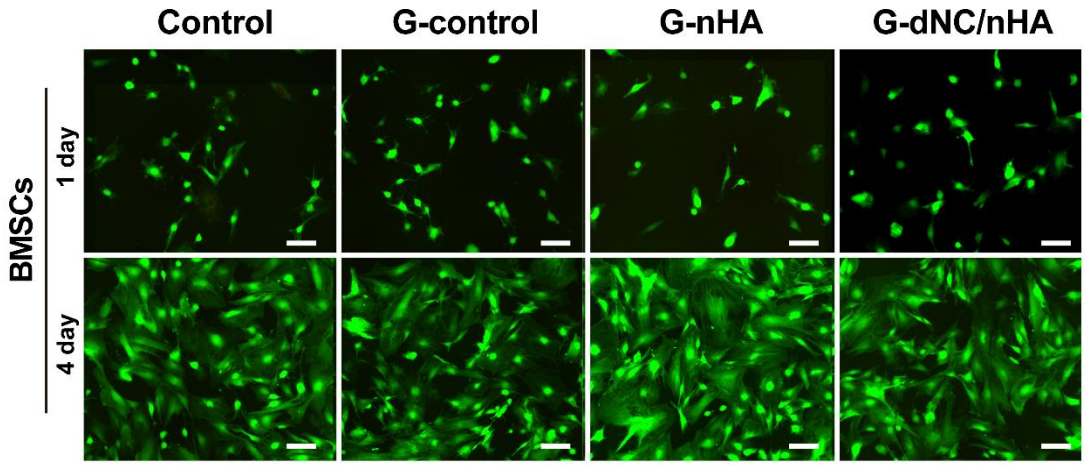

Figure S10. Images of Live/Dead staining were captured after co-culturing BMSCs with various samples for 1 and 4 days. (Live cells: green fluorescence, dead cells: red fluorescence. Scale bar:100 μm.

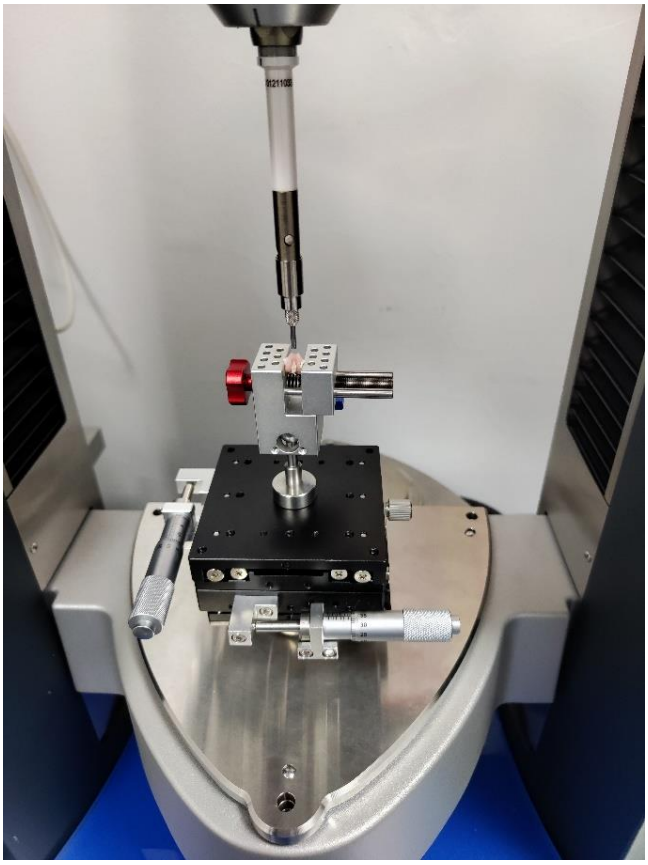

Figure S11. The image of mechanical test equipment of normal and repaired cartilage.

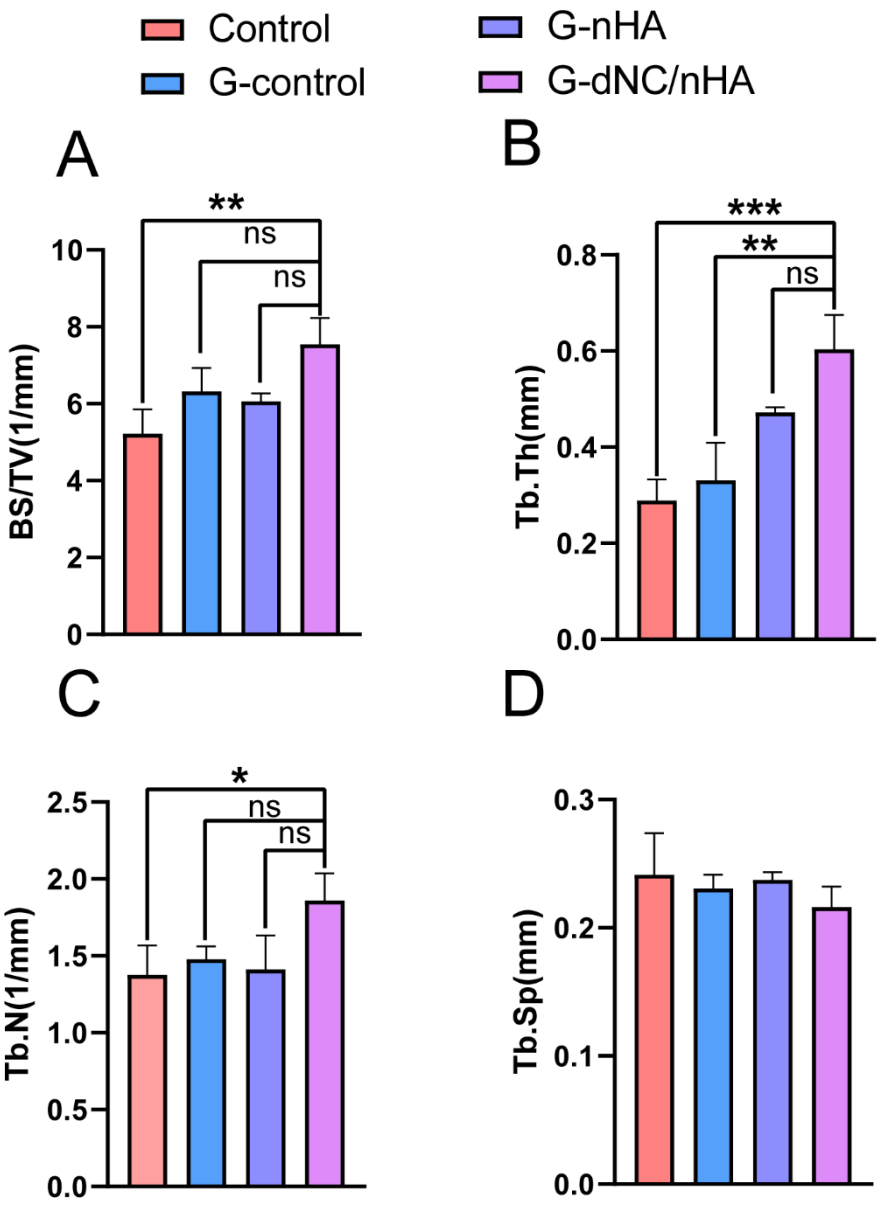

Figure S12 A–D) Images of bone surface fraction (BS/TV), trabecular thickness (Tb.Th), trabecular number (Tb.N), and trabecular separation (Tb.Sp) (n=3). All data were analyzed by one-way ANOVA, and error bars indicate mean ± SD, *p < 0.05, **p < 0.01, and ***p < 0.001. "ns" represents no significance.

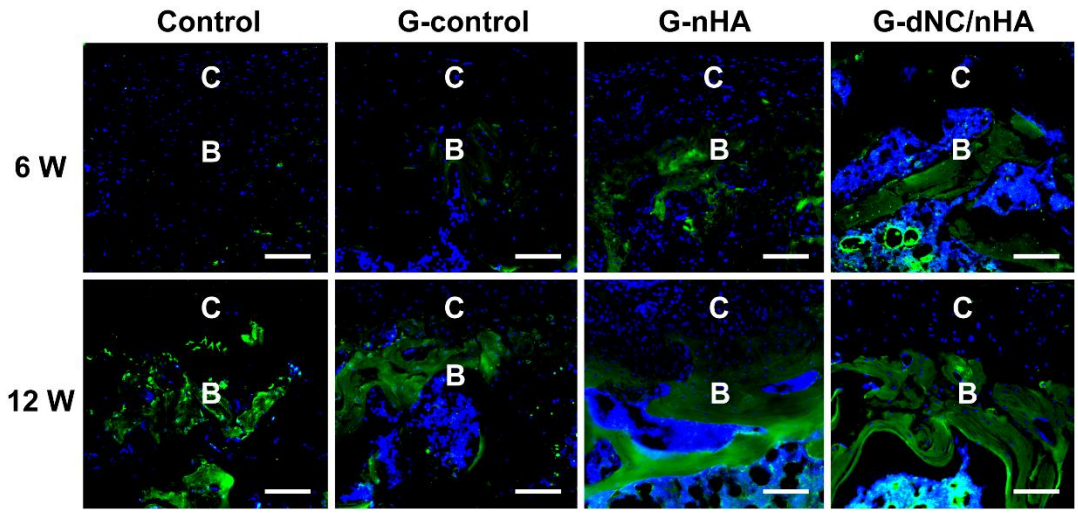

Figure S13. Immunofluorescence (IF) images of osteocalcin (OCN, green) of the repaired tissue at 6 and 12 weeks. C: cartilage; B: bone. Scare bar: 100 μm.

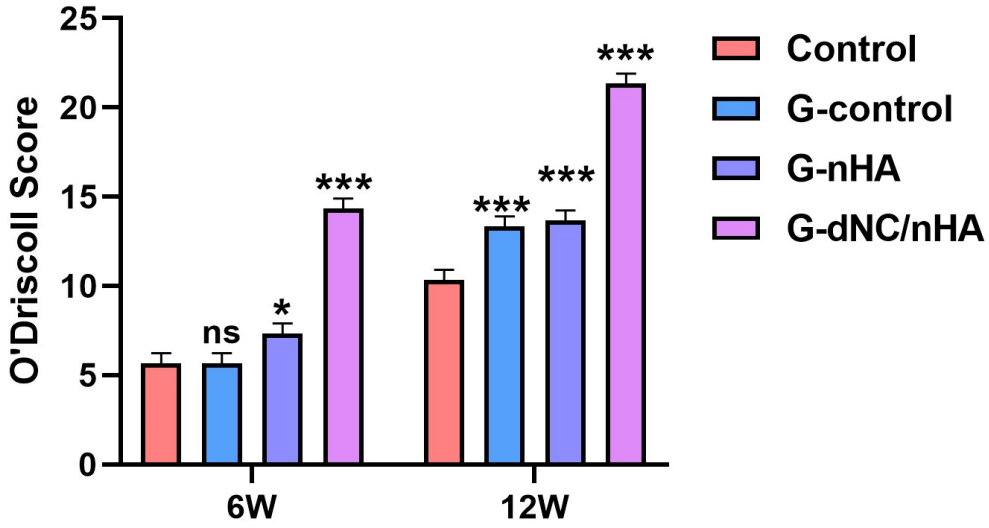

Figure S14. According to the O'Driscoll scoring criteria, histological repair scores were analyzed to assess the effectiveness of cartilage repair in each study group at 6 and 12 weeks. The data were analyzed by one-way ANOVA analysis, and error bars indicate Mean ± SD, *p<0.05, **p<0.01, ***p<0.001."ns" represented no significance.

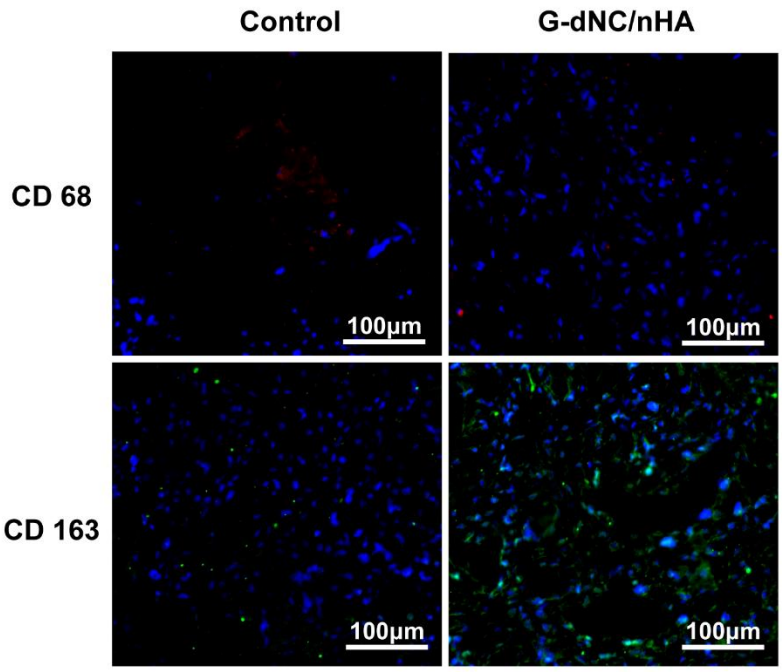

Figure S15. Immunofluorescence staining of macrophage (CD68 red), type 2 macrophage (CD163 green), and DAPI (blue) was utilized to assess the inflammatory and immunomodulatory effects of G-dNC/nHA scaffolds. Scale bar: 100 μm.

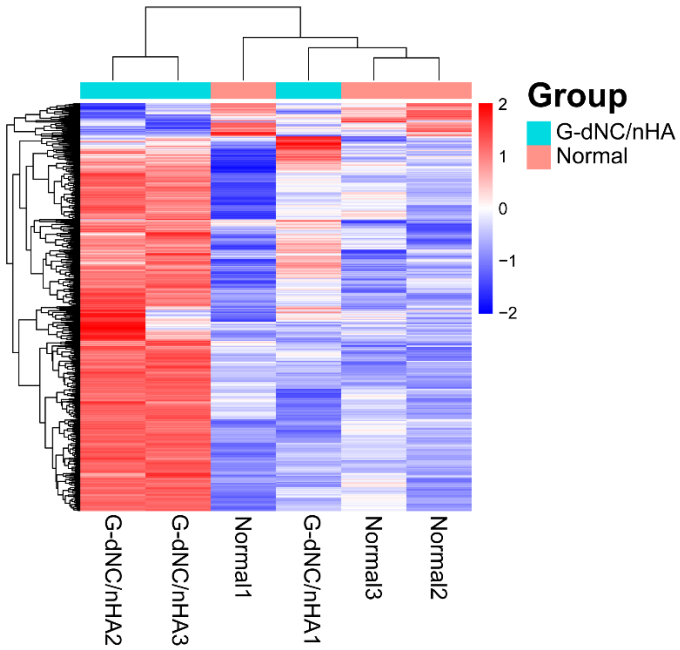

Figure S16. heatmap of the differentially expressed genes (DEGs) in the G-dNC/nHA group and the normal group.

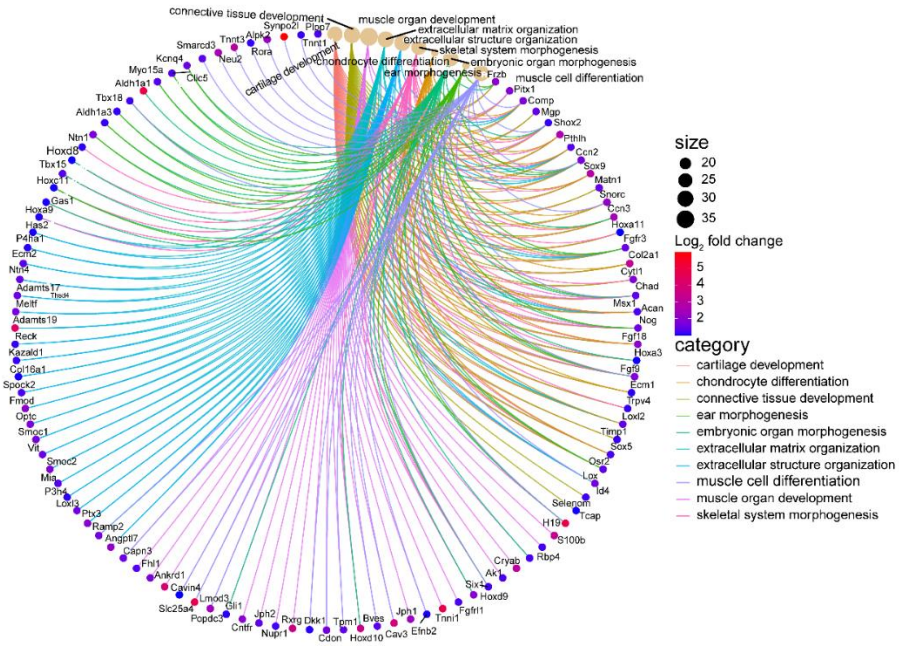

Figure S17. The circular plot of DEGs is mainly associated with the biological process of cartilage development, chondrocyte differentiation, and extracellular matrix organization.

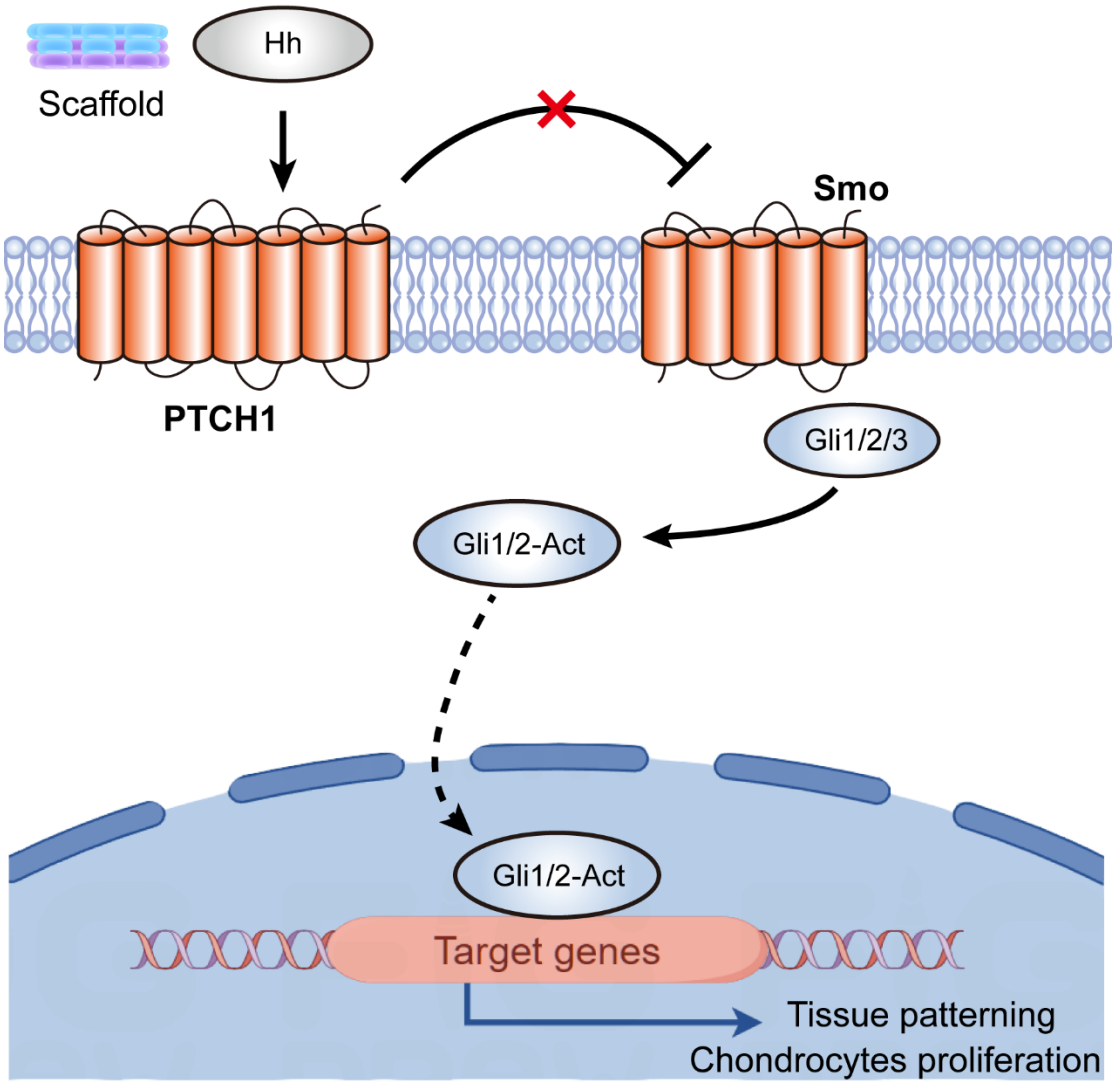

Figure S18. The G-dNC/nHA scaffold promoted osteochondral defect regeneration via activating the Hedgehog signaling pathway. The picture material of the cell nuclear was drawn by Figdraw.

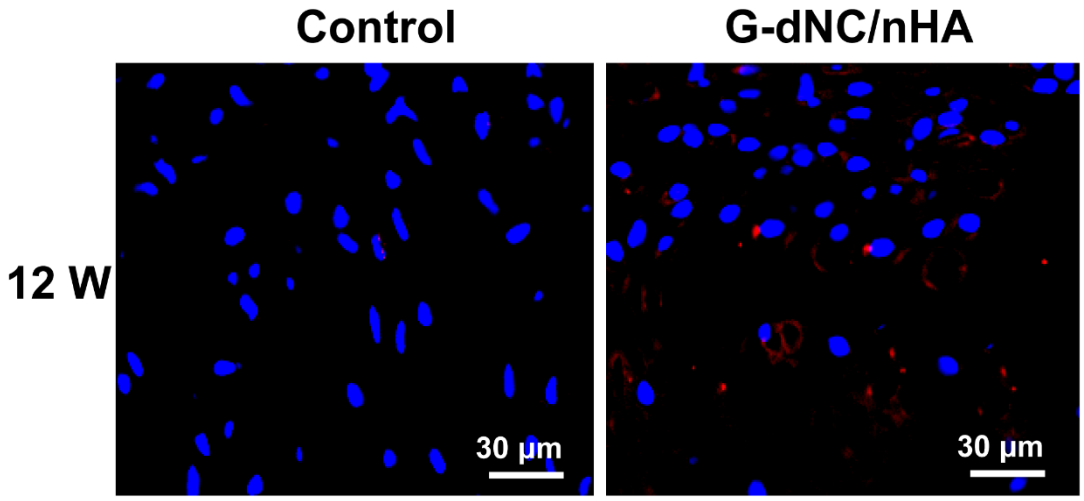

Figure S19. IF images of Gli1 (red) of the repaired tissue at 12 weeks. Scare bar: 100 μm.

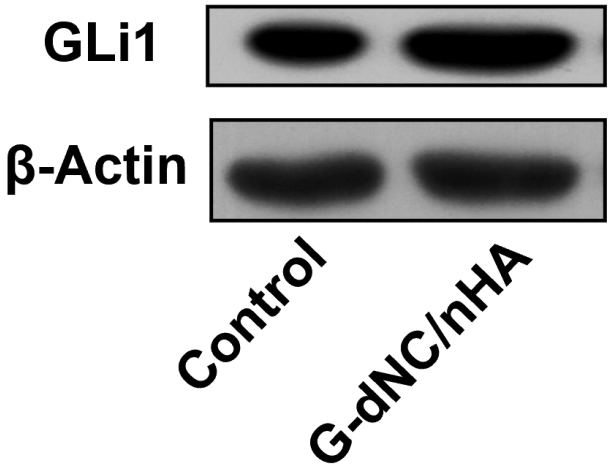

Figure S20 Western blot of Gli1 in Control and G-dNC/nHA groups.

Table S1. 3D printing parameters

Parameters	Value
Nozzle temperature of upper layer inks	25 ℃
Extrusion pressure of upper inks	5-8 psi
Nozzle temperature of lower layer inks	37 ℃
Extrusion pressure of upper inks	15-20 psi
Printing speed	3 mm/s
Height of upper layer inks	0.5 mm
Height of calcified layer (cross-printing layer)	0.5 mm
Height of lower layer inks	1 mm

Tabel S2. Primer sequences of chondrogenic genes.

Gene	Primers	
	Forward (5'-3')	Reverse (5'-3')
RPL4	AGACAATGCGCCGAAACA	TACCACGGGCTTCTTGTCT
Col I	AAGATGTGCCACTCCGACT	AAGATGTGCCACTCCGACT
Col II	ATGGCTGCACGAAACACA	ATGGCTGCACGAAACACA
Col X	CAGGTACCAGAGGTCCCATC	CAGGTACCAGAGGTCCCATC
ACAN	CGAGGAGCAGGAGTTTGTCAAC	ATCATCACCACGCAGTCCTCTC

Tabel S3. Primer sequences of osteogenic genes.

Gene	Primers	
	Forward (5'-3')	Reverse (5'-3')
GAPDH	AAGAAACCCTGGACCACCCAGC	TGGTATTCGAGAGAAGGGAGGG
ALP	CCCGAGTGCTTTGTGTGTGCTG	CCGCCGGTGTTCGTGTGTG
RUNX2	TCTTCCCAAAGCCAGAGCG	TGCCATTCGAGGTGGTCG
Col I	CTCCTGGCAAGAACGGAGATGA	CTCCTTTGGCACCATCCAAACC
OPN	TTGGCTTTGCAGTCTCCTGCGG	AGGCAAGGCCGAACAGGCAAA
OCN	CAGTAAGGTGGTGAATAGACT	GGTGCCATAGATGCGCTTG

Table S4. ICRS macroscopic evaluation of cartilage repair

Categories	Points
Degree of defect repair	
In level with surrounding cartilage	4
75% repair of defect depth	3
50% repair of defect depth	2
25% repair of defect depth	1
0% repair of defect depth	0
Integration to border zone	
Complete integration with surrounding cartilage	4
Demarcating border < 1 mm	3
3/4 of graft integrated, 1/4 with a notable border > 1 mm width	2
1/2 of graft integrated with surrounding cartilage, 1/2 with a notable border > 1 mm	1
From no contact to 1/4 of graft integrated with surrounding cartilage	0
Macroscopic appearance	
Intact smooth surface	4
Fibrillated surface	3
Small, scattered fissures of cracks	2
Several, small or few but large fissures	1
Total degeneration of grafted area	0
Overall repair assessment	
Grade I: normal	12
Grade II: nearly normal	8-11
Grade III: abnormal	4-7
Grade IV: severely abnormal	1-3

Table S5. O'Driscoll scoring system

(a) Nature of the predominant tissue	Score
1 Cellular morphology	
Hyaline articular cartilage	4
Incompletely differentiated mesenchyme	2
Fibrous tissue or bone	0
2 Safranin-O staining of the matrix	
Normal or nearly normal	3
Moderate	2
Slight	1
None	0
(b)Structural characteristics	
3 Surface regularity	
Smooth and intact	3
Superficial horizontal lamination	2
Fissures - 25 to 100 per cent of the thickness	1
Severe disruption. including fibrillation	0
4 Structural integrity	
Normal	2
Slight disruption including cysts	1
Severe disintegration	0
5 Thickness	
100 per cent of normal adjacent cartilage	2
50-100 per cent of normal cartilage	1
0-50 per cent of normal cartilage	0
6 Bonding to the adjacent cartilage	
Bonded at both ends of graft	2
Bonded at one end, or partially at both ends	1
Not bonded	0
(c)Freedom from cellular changes of degeneratio	
7 Hypocellularity	
Normal cellularity	3
Slight hypocellularity	2
Moderate hypocellularity	1
Severe hypocellularity	0
8 Chondrocyte clustering	
No clusters	2
<25 per cent of the cells	1
25-100 per cent of the cells	0
9 Freedom from degenerative changes in adjacent cartilage	
Normal cellularity.no clusters, normal staining	3
Normal cellularity.no clusters, normal staining	2
Mild or moderate hypocellularity, slight staining	1
Severe hypocellularity. poor or no staining	0

Reference

[1] F.H. Chen, K.T. Rousche, R.S. Tuan, Technology Insight: adult stem cells in cartilage regeneration and tissue engineering, Nature Clinical Practice Rheumatology 2(7) (2006) 373-382. https://doi.org/10.1038/ncprheum0216.

[2] Y. Liu, M.B. Chan-Park, A biomimetic hydrogel based on methacrylated dextran-graft-lysine and gelatin for 3D smooth muscle cell culture, Biomaterials 31(6) (2010) 1158-1170. https://doi.org/https://doi.org/10.1016/j.biomaterials.2009.10.040.

[3] J. Gao, X. Ding, X. Yu, X. Chen, X. Zhang, S. Cui, J. Shi, J. Chen, L. Yu, S. Chen, J. Ding, Cell-Free Bilayered Porous Scaffolds for Osteochondral Regeneration Fabricated by Continuous 3D-Printing Using Nascent Physical Hydrogel as Ink, Advanced Healthcare Materials 10(3) (2021) 2001404. https://doi.org/https://doi.org/10.1002/adhm.202001404.

[4] J. Liu, L. Li, H. Suo, M. Yan, J. Yin, J. Fu, 3D printing of biomimetic multi-layered GelMA/nHA scaffold for osteochondral defect repair, Materials & Design 171 (2019) 107708. https://doi.org/https://doi.org/10.1016/j.matdes.2019.107708.

[5] W. Wei, H. Dai, Articular cartilage and osteochondral tissue engineering techniques: Recent advances and challenges, Bioactive Materials 6(12) (2021) 4830-4855. https://doi.org/https://doi.org/10.1016/j.bioactmat.2021.05.011.

[6] H. Yao, T. Li, Z. Wu, Q. Tao, J. Shi, L. Liu, Y. Zhao, Superlarge living hyaline cartilage graft contributed by the scale-changed porous 3D culture system for joint defect repair, Biomedical Materials 17(6) (2022) 064101. https://doi.org/10.1088/1748-605X/ac8a31.